

Article

A Study on the Relationship between Strong Earthquake and Abnormality of Space Static Electricity with Sample

Chong-fu Huang ^{1,*}, Tao Chen ² and Lei Li ^{2,3}

¹ Academy of Disaster Risk Sciences, Faculty of Geographical Science, Beijing Normal University, Beijing (100875), China

² National Space Science Center, Chinese Academy of Sciences, Beijing (100190), China

³ School of Earth and Planetary, University of Chinese Academy of Sciences, Beijing (100049), China

* Correspondence: hchongfu@bnu.edu.cn

Received: November 28, 2023; Received in revised form: December 28, 2023; Accepted: December 28, 2023;
Available online: December 31, 2023

Abstract: It has been observed that, before some strong earthquakes occur, the space static electricity near the ground is abnormal, which might be caused by a large amount of radioactive gas released from the Earth's crust. In this paper, the information diffusion technology for optimally processing small samples is used to analyze 30 cases, and the relationship between magnitude and parameters such as abnormality of space static electricity is constructed. Each case is composed of four observation values: abnormality e , epicenter distance d , impending time t and magnitude m . Using the causal relationship constructed in this paper, the magnitude m of an impending earthquake could be approximately inferred from abnormality e . According to the progress of locking the epicenter and the passage of time, the predicted magnitude could be adjusted in a timely manner. The research results provided in this paper do not eliminate the uncertainty of earthquake occurrence, so that the study is a work of analyzing seismic dynamic risk. Integrating the monitoring information from seismic stations and the physical field information in the air will promote impending earthquake prediction, which is a worldwide scientific challenge.

Keywords: Earthquake; Static Electricity; Abnormal; Information Diffusion; Relationship; Impending Earthquake Prediction

1. Introduction

A plethora of research findings in seismology and geology have provided vital foundations for earthquake intensity zoning and exploration of medium and long-term earthquake forecasts. Additionally, the rich research outcomes in geophysics have significantly aided in understanding the physical processes leading to earthquakes and detecting earthquake precursor information. However, due to the complexities of geological conditions at the occurrence sites of tectonic earthquakes, their analysis remains challenging, often limited to inferences based on seismic activity. Moreover, the geophysical changes originating deep within the earthquake source weaken considerably when reaching the Earth's surface, becoming susceptible to numerous interferences, making it extremely difficult to capture corresponding reliable earthquake precursor information. As of now, the best achievable efforts are limited to providing warnings for areas outside the epicenter before an earthquake strikes, creating ground deformation maps after an earthquake, and

inferring the mechanisms behind the earthquake occurrence. Short-term earthquake prediction remains a global scientific challenge.

Commonly referred to as short-term earthquake prediction, or short-term forecasting, forecasts concerning the timing, location, and magnitude of earthquakes within a 10-day timeframe are the focus of this study. In his work on the Meridian Project and the Honghu Special Research Project, Researcher Chen Tao made an unexpected discovery. He noticed that negative anomalies in atmospheric vertical static electric signals always appeared several hours or tens of hours before seismic ruptures of varying magnitudes. Subsequent investigations revealed that when spatial electric field anomalies occurred, a strong earthquake might occur within a range of 30 to 55 kilometers from the observation site within 2 to 48 hours (Chen et al., 2023) [1]. However, it is not feasible to infer earthquake magnitude, epicenter, or seismic occurrence time solely based on the signals from individual stations.

In this study, we have compiled 30 case records, each comprising four observational values: static electric anomaly value (e), epicentral distance from the observation point (d), short-term forecast time (t), and earthquake magnitude (m). Employing an optimized small-sample information diffusion technique, we have conducted an analysis of the 30 cases and established relationships between earthquake magnitude and static electric anomalies. The goal is to roughly estimate the short-term earthquake magnitude (m) from e values and, after fixing the epicentral distance (d), approximate t for further estimation of m .

2. Information Diffusion Techniques

In the field of communication engineering, "information" refers to something that eliminates stochastic uncertainty, characterized solely by waveform factors without content or value. In modern artificial intelligence theory, information is divided into objective information and perceived information. The former pertains to the "state and its changing mode" presented by the object, while the latter refers to the form, content, and utility of the object's state and its changing mode as perceived by the subject (Zhong, 2018) [2]. In the context of information diffusion techniques, observational values from sample points are considered as information that has already been perceived.

Information diffusion, also known as information dissemination, involves expanding point-like perceived information into aggregated information, aiming to gain understanding beyond the realm of perceived information. It is an inherent human instinct to use limited knowledge to comprehend an infinite world. Information diffusion is distinct from association, as it does not involve recalling other related people or things due to someone or something. Additionally, information diffusion is not the same as information propagation, which involves the exchange of information among individuals, organizations, and groups through symbols and media. In recent years, some literature has referred to "information propagation" as "information diffusion," intending to leverage a plethora of mathematical tools to study information dissemination, while the essence of propagation remains unchanged.

Information diffusion techniques are based on the principles of optimizing the processing of small samples (Huang, 1997) [3]: when estimating a relationship with incomplete data, there must be a reasonable diffusion method that can transform an observation with no geometric magnitude into a set value, filling the partial defects caused by incompleteness to improve non-diffusion estimates.

This principle holds not only in probability space but also in geometric space (Makó, 2005) [4]. This means that information diffusion techniques can be extended to geographical space to fill data gaps in geographic units, converting incomplete spatial data sets into complete ones (Huang, 2021) [5]. Extensive applications have confirmed the universality of information diffusion techniques. Particularly for small-sample problems in complex nonlinear cases, information diffusion techniques not only yield smaller prediction errors but also ensure that there are no cases with prediction errors significantly smaller than baseline errors, thereby ensuring the validity of the predictions (Huang, 2020) [6]. In contrast, neural network models that can highly fit training samples may have small baseline errors, but their prediction errors can sometimes be nearly an order of magnitude higher than baseline errors, rendering them unsuitable for interpolating complex phenomena (Huang and Zhang, 2022) [7].

As the objective of information diffusion is to unearth as much useful information as possible to improve system identification accuracy, this technique is also referred to as fuzzy information optimization. The simplest diffusion technique is the linear information distribution method, commonly known as the information distribution method. The most widely applied diffusion technique is the normal information diffusion, also known as the normal diffusion method.

Let $X = \{x_1, x_2, \dots, x_n\}$ be a sample observed from an experiment, and $U = \{u_1, u_2, \dots, u_I\}$ be a discrete universe of X (a domain of x), called monitoring space in the information diffusion theory, also called controlling space particularly to the information distribution method. Usually, the minimum monitoring point u_1 and maximum monitoring point u_I are selected from X by Eq. (1), and other points in the monitoring space are chosen equidistantly.

$$u_1 = \min_{1 \leq i \leq n} \{x_i\}, \quad u_I = \max_{1 \leq i \leq n} \{x_i\}. \quad (1)$$

There is an asymptotical optimal formula (2) to choose the number I of controlling points. Theoretically, there should be as many monitoring points as possible for normal diffusion, but they are usually selected based on the accuracy of the observation points because too many monitoring points do not help much to improve the recognition accuracy except increasing the workload of computation.

$$I = 1 + 1.87(n-1)^{2/5} \quad (2)$$

In information distribution, we say that the information carried by an observation x is distributed to the two closest controlling points to the x . The amount of information distributed calculated by Eq. (3) is known as linear information distribution.

$$\mu(x, u) = \begin{cases} (1 - \frac{|x-u|}{\Delta}), & |x-u| \leq \Delta, \\ 0, & \text{其它.} \end{cases} \quad (3)$$

where Δ is the distance between controlling points.

In the normal diffusion, we say that the information carried by an observation x is diffused to all monitoring points in the form of a normal distribution. The amount of information obtained by monitoring point u from observation x is calculated by Eq. (4).

$$\mu_x(u) = \exp[-\frac{(x-u)^2}{2h^2}], \quad x \in X, u \in U. \quad (4)$$

The asymptotically optimized diffusion coefficient h for normal diffusion can be calculated using Eq. (5) (Huang, 2012) [8].

$$h = \begin{cases} 0.8146(b-a), & n=5; \\ 0.5690(b-a), & n=6; \\ 0.4560(b-a), & n=7; \\ 0.3860(b-a), & n=8; \\ 0.3362(b-a), & n=9; \\ 0.2986(b-a), & n=10; \\ 2.6851(b-a)/(n-1), & n \geq 11. \end{cases} \quad (5)$$

where $b = \max_{1 \leq i \leq n} \{x_i\}$, $a = \min_{1 \leq i \leq n} \{x_i\}$.

The $\mu(x, u)$ and $\mu_x(u)$ in Eq. (3) and Eq. (4) are both called information gain obtained by monitoring point u from observation x , although they are produced in different ways. The $\mu_x(u)$ has a wider range of applications than the $\mu(x, u)$.

3. Constructive Causation

The sample X formed by the 30 cases is denoted as in (6), where each observation includes four parameters: electrostatic anomaly e , epicentral distance from the observation point d , proximity time t and earthquake magnitude m :

$$X = \{x_1, x_2, \dots, x_n\} = \{(e_1, d_1, t_1, m_1), (e_2, d_2, t_2, m_2), \dots, (e_{30}, d_{30}, t_{30}, m_{30})\}. \quad (6)$$

The dimensions of these parameters are -kV/m, kilometer, hour, and Richter magnitude, respectively. For example, the 9th case $x_9 = (2.75, 50, 7, 7.9)$ means that, a 7.9 magnitude earthquake occurred 7 hours after observing the maximum electric field anomaly of 2.75, which was observed at an observation point 50 kilometers from the epicenter.

V/m is the unit of electric field strength, which is defined as the strength of the electric field between two parallel charged plates spaced 1 m apart, if the measured voltage is 1 volt, the strength of the electric field between them is 1 V/m. The strength of electrostatic forces in space is measured using an atmospheric electric field meter, which uses the principle of induced charge generated by a conductor in an electric field to measure it. Under normal clear-sky conditions, the bottom of the ionosphere is positively charged, the surface is negatively charged, and the space electrostatic force detected by near-surface instruments is positive, about several hundred V/m; when thunderstorm clouds or other charged clouds appear, a negative electric field is formed locally below the clouds. If a negative electric field occurs on a clear day, we call it an atmospheric electrostatic anomaly, which may be caused by various crustal movements during the pre-seismic phase, which lead to the fragmentation or melting of rocks, the dissolution or phase transformation of minerals, and the release of large quantities of daughter isotopes of the decaying parent isotopes of some radioactivity retained in certain minerals or rocks.

According to the range of observed values of each parameter in the sample X and the sample capacity $n=30$, we adopt U , V , W and Z in Eq. (7) as the monitoring spaces for e , d , t and m ,

respectively.

$$\begin{cases} U = \{u_1, u_2, \dots, u_8\} = \{0.28, 2.669, 5.057, 7.446, 9.834, 12.223, 14.611, 17\}; \\ V = \{v_1, v_2, \dots, v_8\} = \{11, 284.286, 557.571, 830.857, 1104.143, 1377.428, 1650.714, 1924\}; \\ W = \{w_1, w_2, \dots, w_8\} = \{2.5, 8.743, 14.986, 21.229, 27.471, 33.714, 39.957, 46.2\}; \\ Z = \{z_1, z_2, \dots, z_8\} = \{3, 3.7, 4.4, 5.1, 5.8, 6.5, 7.2, 7.9\}. \end{cases} \quad (7)$$

The diffusion coefficients for e, d, t and m are calculated by using Eq. (5), shown in (8).

$$\begin{cases} h_e = 1.548; \\ h_d = 177.1; \\ h_t = 4.046; \\ h_m = 0.4537. \end{cases} \quad (8)$$

The 4-dimensional information diffusion Eq. (9) is used to diffuse information of any observation $x_i = (e_i, d_i, t_i, m_i)$, $i = 1, 2, \dots, 30$, to all monitoring points $u \in U, v \in V, w \in W, z \in Z$.

$$\mu_{x_i}(u, v, w, z) = \exp\left[-\frac{(e_i - u)^2}{2h_e^2} - \frac{(d_i - v)^2}{2h_d^2} - \frac{(t_i - w)^2}{2h_t^2} - \frac{(m_i - z)^2}{2h_m^2}\right]. \quad (9)$$

To guarantee every observation to be equally important for the constructive causation, we use Eq. (10) to normalize the information diffused by the sample points x_i .

$$\rho_i(u, v, w, z) = \begin{cases} \mu_{x_i}(u, v, w, z)/s, \\ s = \sum_{j,k,l,g=1}^{30} \mu_{x_j}(u_j, v_k, w_l, z_g). \end{cases} \quad (10)$$

Then, Eq. (11) is used to sum the information gains obtained from the diffusion of 30 sample points for each monitoring point respectively, and the Primary Information Distribution (Q) of 30 cases is obtained (Eq. (12)).

$$q(u, v, w, z) = \sum_{i=1}^{30} \rho_i(u, v, w, z). \quad (11)$$

$$Q = \{q(u, v, w, z)\}_{U \times V \times W \times Z}. \quad (12)$$

Each q in Eq. (12) is also called an information gain, but from the sample X rather than a sample point x . Theoretically, the sum of all gains in Q is equal to the size of the of sample in (6), i.e., 30.

The Q is a 4-dimensional matrix that can only be written down to 2 dimensions. For example, fixing $v_2 = 284.286$ and $w_3 = 14.986$, this Q can be expressed as:

$$Q(v_2, w_3) = \begin{matrix} & \begin{matrix} z_1 & z_2 & z_3 & z_4 & z_5 & z_6 & z_7 & z_8 \end{matrix} \\ \begin{matrix} u_1 \\ u_2 \\ u_3 \\ u_4 \\ u_5 \\ u_6 \\ u_7 \\ u_8 \end{matrix} & \begin{bmatrix} 0.004 & 0.028 & 0.176 & 0.343 & 0.165 & 0.067 & 0.027 & 0.020 \\ 0.002 & 0.017 & 0.085 & 0.144 & 0.066 & 0.024 & 0.013 & 0.020 \\ 0.000 & 0.002 & 0.007 & 0.006 & 0.002 & 0.001 & 0.002 & 0.004 \\ 0.000 & 0.000 & 0.000 & 0.000 & 0.001 & 0.000 & 0.000 & 0.000 \\ 0.000 & 0.000 & 0.000 & 0.001 & 0.006 & 0.004 & 0.000 & 0.000 \\ 0.000 & 0.000 & 0.000 & 0.001 & 0.006 & 0.004 & 0.000 & 0.000 \\ 0.000 & 0.000 & 0.000 & 0.000 & 0.001 & 0.003 & 0.008 & 0.002 \\ 0.000 & 0.000 & 0.000 & 0.000 & 0.000 & 0.008 & 0.025 & 0.008 \end{bmatrix} \end{matrix} \quad (13)$$

Taking the maximum gains with respect to the monitoring spaces U , V , W and Z in Eq. (7), respectively, we normalize the gains of Q in Eq. (13) to generate four marginal distributions. The normalization process is called "maximum - dividing". For example, the gain of the monitoring point z_1 of the space Z for parameter m is normalized by Eq. (14).

$$\begin{cases} q_{z_1}(u, v, w, z_1) = q(u, v, w, z_1)/a_{z_1}, \\ a_{z_1} = \max_{1 \leq j, k, l \leq 30} \{q(u_j, v_k, w_l, z_1)\}. \end{cases} \quad (14)$$

The four marginal distributions are then subjected to a miniaturization operation for constructing a fuzzy relation R on U , V , W , and Z . Then, for any u_j , v_k , and w_l , taking the maximum value of all elements on monitoring points z_1, z_2, \dots, z_8 to normalize R by division, we obtain an approximate causal relationship $R_{e,d,t \rightarrow m}$ with abnormality e , epicenter distance d , impending time t as inputs and magnitude m as output. For example, fixing $v_2=284.286$ and $w_3=14.986$, the approximate causal relationship is shown in Eq. (15).

$$R_{e,d,t \rightarrow m}(v_2, w_3) = \begin{matrix} & \begin{matrix} z_1 & z_2 & z_3 & z_4 & z_5 & z_6 & z_7 & z_8 \end{matrix} \\ \begin{matrix} u_1 \\ u_2 \\ u_3 \\ u_4 \\ u_5 \\ u_6 \\ u_7 \\ u_8 \end{matrix} & \begin{bmatrix} 0.004 & 0.033 & 0.212 & 0.414 & 0.199 & 0.081 & 0.033 & 0.024 \\ 0.005 & 0.047 & 0.239 & 0.360 & 0.186 & 0.069 & 0.038 & 0.057 \\ 0.006 & 0.095 & 0.293 & 0.230 & 0.100 & 0.034 & 0.064 & 0.179 \\ 0.002 & 0.039 & 0.095 & 0.084 & 0.411 & 0.246 & 0.040 & 0.084 \\ 0.000 & 0.000 & 0.001 & 0.077 & 0.564 & 0.339 & 0.019 & 0.000 \\ 0.000 & 0.000 & 0.001 & 0.074 & 0.547 & 0.334 & 0.037 & 0.006 \\ 0.000 & 0.000 & 0.000 & 0.006 & 0.047 & 0.199 & 0.574 & 0.174 \\ 0.000 & 0.000 & 0.000 & 0.000 & 0.005 & 0.188 & 0.618 & 0.188 \end{bmatrix} \end{matrix} \quad (15)$$

4. Approximate Estimation of Earthquake Magnitude

The magnitude m of a critical earthquake can be approximately inferred by e , d , t , using the causal relationship $R_{e,d,t \rightarrow m}$ constructed from many cases.

If and only if the inputs e , d , and t are exactly equal to a certain element of U , V , and W , respectively, the critical earthquake magnitude m can be inferred directly from $R_{e,d,t \rightarrow m}$. For example, when $e=u_1=0.28$, $d=v_2=284.286$, and $t=w_3=14.986$, the possibility distribution of the critical earthquake magnitude m in the monitoring space Z is just the first row of $R_{e,d,t \rightarrow m}(v_2, w_3)$, shown in Eq. (16).

$$\begin{aligned} \text{Poss}(u_1, v_2, w_3) &= (r(u_1, v_2, w_3, z_1), r(u_1, v_2, w_3, z_2), \dots, r(u_1, v_2, w_3, z_8)) \\ &= (0.004, 0.033, 0.212, 0.414, 0.199, 0.081, 0.033, 0.024) \end{aligned} \quad (16)$$

Because the maximum possibility (i.e., 0.414) is on monitoring point z_4 and $z_4 = 5.1$ in Eq. (7), we roughly infer that the earthquake that will occur is about magnitude 5.1. Considering the other possibilities in Eq. (16), we more approximately infer the magnitude using the information concentration formula in Eq. (17).

$$m = \frac{\sum_{i=1}^8 r^2(u_1, v_2, w_3, z_i)z_i}{r^2(u_1, v_2, w_3, z_i)} = \frac{0.004 \times 0.004 \times 3 + \dots + 0.024 \times 0.024 \times 7.9}{0.004 \times 0.004 + \dots + 0.024 \times 0.024} = 5.13. \quad (17)$$

When the inputs e , d , and t are not exactly equal to one of monitoring points in U , V , and W ,

respectively, we use Eq. (3) to distribute the information carried by each input to the two closest controlling points. Then, use the max-min operation to infer the possibility distribution on monitoring space Z. For example, when $e=13.5$, $d=v_2=284.286$ and $t=w_3=14.986$, i.e., e (abnormality of space static electricity) is not exactly equal to one of monitoring points in U , with the distance between controlling points of U , $\Delta=u_7-u_6=14.611-12.223=2.388$. The information is distributed to $u_6=12.223$ and $u_7=14.611$ by Eq. (18):

$$\mu(13.5, u_6) = 1 - \frac{13.5 - 12.223}{2.388} = 0.465, \quad \mu(13.5, u_7) = 1 - \frac{14.611 - 13.5}{2.388} = 0.535 \quad (18)$$

Using the max-min operation with R , we obtain a possibility distribution on controlling space Z:

$$\begin{aligned} \text{Poss}(13.5, v_2, w_3) &= (r(13.5, v_2, w_3, z_1), r(13.5, v_2, w_3, z_2), \dots, r(13.5, v_2, w_3, z_8)) \\ &= (0, 0, 0.001, 0.074, 0.465, 0.334, 0.535, 0.174) \end{aligned} \quad (19)$$

The information is centralized to infer the magnitude of the proximate earthquake:

$$m=6.63.$$

In most cases, we first observe the electrostatic anomaly e , but we do not know the distance d from the epicenter of the observation point and the time of proximity t . In this case, it is sufficient to use the causality $R_{e \rightarrow m}$, which is built from the historical data of e and m in 30 cases, to infer the magnitude of the proximity magnitude m more roughly from e .

Similarly, the causal relation $R_{e \rightarrow t}$, established from the historical data of e and t in 30 cases, can be used to make a rough estimate of the seismic time t from e . From the observed electrostatic anomaly e and the rough estimate of the seismic time t , the seismic magnitude m can be further estimated using the causal relation $R_{e, t \rightarrow m}$.

When the roughly estimated magnitude reaches the strong earthquake level, mobile technologies such as unmanned aerial vehicles are used, and factors such as the drift of the electrostatic field with the wind are considered to lock the electrostatic anomaly field in time, calculate the center of the field, and speculate the epicenter while estimating the distance from the epicenter of the observation point, d . At this time, using the causality relationship $R_{e, d, t \rightarrow m}$, the magnitude m can be further speculated more closely from e , d , and an adjusted t . The adjustment in the value of t is such that, with the expenditure of a certain amount of time to speculate the epicenter, the proximity time t inferred from e should be increased appropriately.

5. Application of Forecasting Program PreQuake

The results of the above research have been solidified in the application program PreQuake, which provides a full service to users. PreQuake is written with 690 lines in Fortran language, which does not rely on any commercial software such as MathLab, and is completely self-contained, making it easy to be embedded in relevant systems for real-time pro-earthquake forecasting.

A user can directly type e , d , and t to predict the magnitude of the seismic magnitude m by PreQuake, also allow to just use e or d and t to predict m . The e , d , and t typed in the program can be used to predict the magnitude of the earthquake.

In PreQuake, the typed e , d , and t are read as variables E0, D0, and T0, respectively, and the predicted magnitude m is output as variable M0. The range of values of these variables is determined by the monitoring space of Eq. (7), i.e., [0.280, 17.000] kV/m, [11, 1924] km, [2.5, 46.2] h

and [3, 7.9] Richter magnitude, respectively. They are determined by 30 cases. In other words, when more cases are available to construct the original information distribution in Eq. (12), updating PreQuake can improve the speculative accuracy.

5.1. Inferring the Magnitude of a Critical Earthquake by Directly Typing in 3 Parameters

Double click the left mouse button on PreQuake to bring up the interface shown in Figure 1.

Type in the number 1, the system prompts "Please type in E0, D0, T0, separated by commas". We type 17, 250, 23, and get the result: E0, D0, T0: 17.000 250.000 23.000. Then the inferred earthquake magnitude is $M_0=7.20$. That is to say, the program PreQuake infers $m=7.2$ by $e=17$, $d=250$, $t=23$. At the same time, the program will output a file PREQUAKE.TXT to record the information as shown in Figure 2.

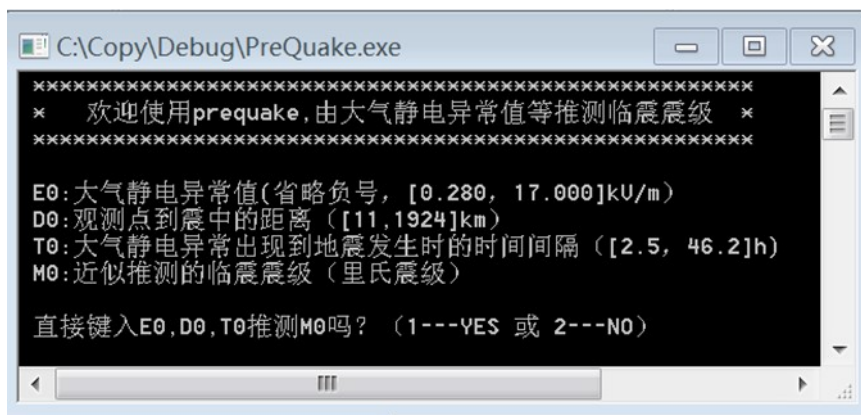


Figure 1. The first appearance of the interface of PreQuake program.

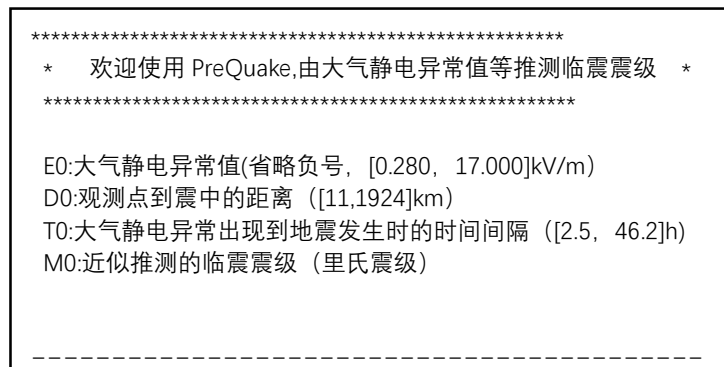


Figure 2. Results are stored in file PREQUAKE.TXT from PreQuake program.

Please note two points when typing information for running PreQuake: (1) Answer a question with numbers 1 or 2, not Y or N, because the logical judgment of the program does not accept string variables; (2) Can only type English character commas "," (half-width form), not Chinese character commas "，" (full-width form).

5.2. Inferring the Magnitude of a Critical Earthquake by Typing in 1 or 2 Parameters

When the interface in Figure 1 appears, type in the number 2, and type in the atmospheric static anomaly after the screen prompts, "Please type in E0 to infer M0: (omit the negative sign, [0.280, 17.000] kV/m)". For example, by typing the number 11, PreQuake predicts a critical
DOI: <https://doi.org/10.54560/jracr.v13i4.410>

magnitude of 5.99. At this point, the program pauses so that the user can view the results, as shown in Figure 3.

After pressing the Enter key, you can choose whether to approximate the proximity time T0 with E0. Next, you can also choose whether to approximate the proximity magnitude with E0 and T0. If we both choose yes (both type the number 1), the program outputs the file shown in Figure 4.

When the anomalous electric field distribution is measured by mobile technologies such as unmanned aerial vehicles, and the epicenter is inferred accordingly, and the epicenter distance is estimated from the surface, the work of inferring the magnitude of the earthquake can be completed by keying in the value of D0 according to the prompts of the system.

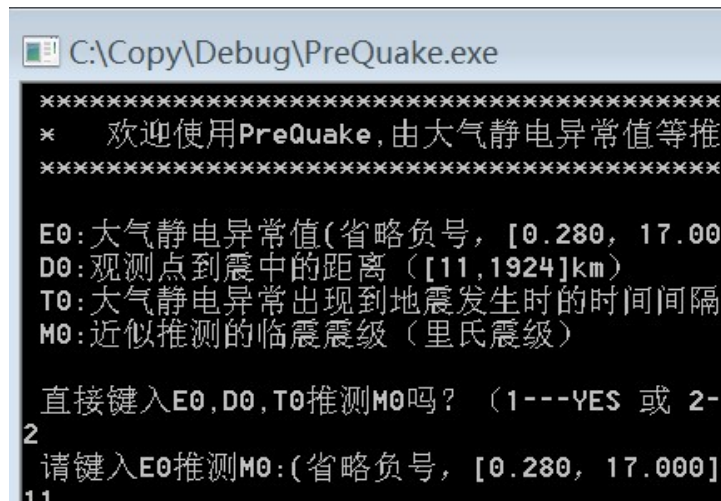


Figure 3. Proseismic magnitude M0 inferred from atmospheric electrostatic anomaly E0.

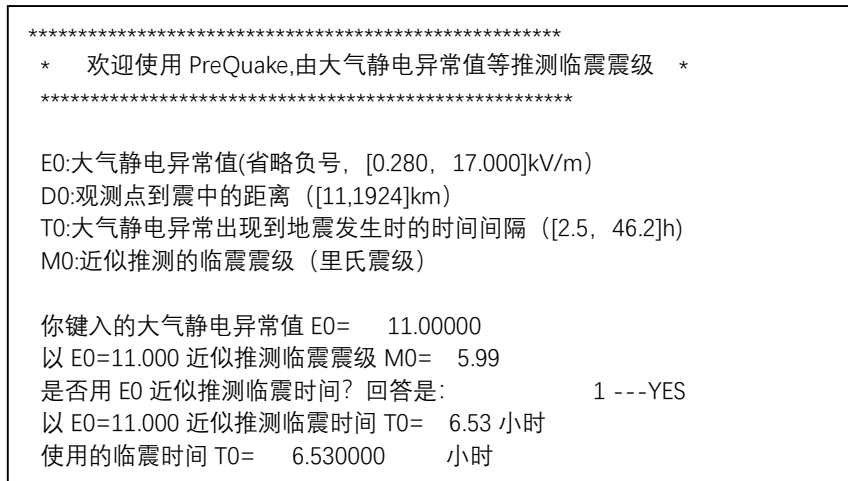


Figure 4. Key in two parameters and save the results in PREQUAKE.TXT.

6. Conclusion and Discussion

Short-range earthquake forecasting is a worldwide scientific problem. With current theories and methods, any prediction formula derived from mathematical and physical equations has no practical value. The crustal deformation, geomagnetic geoelectricity and underground fluids

monitored by traditional seismic stations are not enough to support short-term earthquake forecasting.

During the proximity phase of a major earthquake, critical changes in the crustal structure near the epicenter region produce a large number of rock microfractures, and the channels between rock crevices are likely to connect with each other and release gases containing trace amounts of radioactive elements (e.g., radon, thorium, etc.) into the air through soil crevices, where radioactive isotopes continue to decay in the process of dispersing into the air, in particular, producing alpha-particles of radioactive ionizing radiation. This fills the atmosphere with an unusually large number of positive and negative ions, and these unusually large numbers of positive and negative ions may produce polarized electric fields that are opposite to those of the atmosphere on a clear day and are monitored by instruments. Combined with the anomalies monitored by seismic stations, approximating the magnitude and duration of the proximity earthquake from the spatial electrostatic anomalies will help to solve the problem of short-range earthquake forecasting.

Destructive earthquakes are complex geologic-geophysical processes occurring at a depth of 20-30 kilometers below the ground, and the inaccessibility of this depth makes it impossible to validate assumptions such as the boundary conditions of the relevant differential equations by experimental or observational means, and it is impossible to establish formulas that can accurately forecast earthquakes using mathematical-physical equations.

Summarizing the precursors of earthquakes by statistical methods has almost become the only way to forecast short-term earthquakes. However, anomalies in physical quantities such as crustal deformation, geomagnetic geoelectricity, and subsurface fluids are so far removed from the statistics of the occurrence of earthquakes that their use to forecast earthquakes has too low a success rate. No country currently allows the use of these physical quantities to issue earthquake forecasts to the public. Combining spatial electrostatic anomalies might improve forecast success.

In addition to the choice of physical quantities determining the forecast success rate, the statistical method also affects the success rate. The magnitude m is clearly not linearly related to the electrostatic anomaly e , the epicenter distance d of the observation point, and the time of proximity t . Even with more cases, it is not possible to use ternary linear regression to predict m . Using the quantile regression in nonparametric statistics, it is not only difficult to solve the problem of multidimensional variable points, but also cannot avoid the choice of model in segmented regression.

The information diffusion technique not only is suitable for constructing any nonlinear statistical relationship in multidimensional, but also has the characteristic of optimally dealing with small samples. Therefore, the relationship between strong earthquakes and parameters such as spatial electrostatic anomalies can be constructed even when there are not many sample points, which effectively improves the forecast success rate.

With the increase of sample size and the inclusion of parameters such as crustal deformation, geomagnetic geoelectricity and subsurface fluids, important progress is expected in short-range earthquake forecasting with information diffusion techniques.

Funding: This research received no external funding.

Conflicts of Interest: The authors declare no conflict of interest.

References

- [1] Chen T, Li L, Zhang X, et al. Possible Locking Shock Time in 2-48 Hours. *Applied Sciences*, **2023**, 13(2): 813. DOI: <https://doi.org/10.3390/app13020813>.
- [2] Zhong Y X. Mechanistic Artificial Intelligence Theory - A Generalized Artificial Intelligence Theory. *Journal of Intelligent Systems*, **2018**, 13(1): 2-18.
- [3] Huang C F. Principle of information diffusion. *Fuzzy Sets and Systems*, **1997**, 91(1): 69-90. DOI: [https://doi.org/10.1016/S0165-0114\(96\)00257-6](https://doi.org/10.1016/S0165-0114(96)00257-6).
- [4] Makó Z. Approximation with diffusion-neural-network. *Proceedings of the 6th International Symposium of Hungarian Researchers on Computational Intelligence*, Budapest, Hungary, **2005**: 18-19.
- [5] Huang C F. Geospatial information diffusion based on self-learning discrete regression, *Journal of Environmental Informatics*, **2021**, 38(2): 93-105. DOI: <https://doi.org/10.3808/jei.202000439>.
- [6] Huang C F. Two judging criteria to check validity of a model for filling gaps caused by incomplete geospatial data. *Environmental Research*, **2020**, 186: 109401. DOI: <https://doi.org/10.1016/j.envres.2020.109401>.
- [7] Huang C F, Zhang X W. Empirical study on geospatial information diffusion technology - A case study of flood disaster in Santai County, Sichuan Province. *Disaster Science*, **2022**, 37(2): 89-101.
- [8] Huang C F. *Natural Hazard Risk Analysis and Management*. Science Press: Beijing, China, **2012**.



Copyright © 2023 by the authors. This is an open access article distributed under the CC BY-NC 4.0 license (<http://creativecommons.org/licenses/by-nc/4.0/>).

(Executive Editor: Wen-jun Li)